

# The sPHENIX Experiment at RHIC and the INTT silicon detector

Y. Akiba,<sup>\*1</sup> A. Enokizono,<sup>\*1</sup> T. Kondo,<sup>\*2</sup> C. M. Kuo,<sup>\*3</sup> T. Hachiya,<sup>\*4</sup> S. Hasegawa,<sup>\*5</sup> B. Hong,<sup>\*6</sup> R. S. Lu,<sup>\*7</sup> I. Nakagawa,<sup>\*1\*8</sup> R. Nouicer,<sup>\*9</sup> G. Nukazuka,<sup>\*1</sup> M. Shimomura,<sup>\*4</sup> and X. Wei<sup>\*10</sup>

The sPHENIX experiment is a new experiment and its new detector of Relativistic Heavy Ion Collider (RHIC). The construction of the sPHENIX detector was completed by April of 2023 and its new detector subsystems were commissioned using  $\sqrt{s_{NN}} = 200$  GeV Au+Au collision. The Japanese group of sPHENIX led by RIKEN is responsible for the construction and operation of a silicon tracker (INTT), which is one of three tracking detectors of the sPHENIX detector complex. The INTT detector successfully demonstrated its design performance from the commissioning data. The sPHENIX experiment will start taking physics data of polarized proton+proton and Au+Au collision data at  $\sqrt{s_{NN}} = 200$  GeV in 2024.

## 1 Introduction

When two heavy atomic nuclei collide at high energy, a new form of matter with very high energy density and temperature is formed. This matter is called quark gluon plasma (QGP). It was discovered that QGPs are produced in collisions of heavy atomic nuclei such as Au+Au collisions at RHIC in Brookhaven National Laboratory (BNL). Later it was confirmed that QGPs are also produced in nuclear collisions at the Large Hadron Collider (LHC) in CERN. The properties of the QGP are currently being investigated at RHIC and the LHC.

The sPHENIX<sup>1)2)</sup> is a second generation experiment and its detector at RHIC. It is an upgrade of the PHENIX experiment<sup>3)</sup>. The sPHENIX is to complete the scientific mission of RHIC in study of QGP and the spin structure of the proton. The physics goals of sPHENIX are illustrated in Fig. 1<sup>a)</sup>. They are:

- (1) Measurement of hadron jets, direct photons, and heavy quarks and study of parton energy loss in

the QGP

- (2) Measurement of the Upsilon particles and temperature of the QGP
- (3) Measurement of jet substructure and the study of parton-QGP interaction
- (4) Study of the spin structure of the proton

High-energy partons (quarks or gluons) lose their energy as they pass through the QGP. The energetic partons then break up into a jet of many energetic hadrons concentrated in a narrow angular region. Therefore, measurements of hadron jets are very useful for elucidating the energy loss of partons in the QGP. The interaction of partons with the QGP medium can also be studied based on the measurement of jet substructures. For these purposes, the sPHENIX detector is designed to measure hadron jets, high transverse momentum ( $p_T$ ) hadrons, and high-energy photons over a wide energy range. The broad kinematic range of  $p_T$  covered by the sPHENIX is depicted in Fig. 2.

Upsilon particles ( $\Upsilon(1S)$ ,  $\Upsilon(2S)$ ,  $\Upsilon(3S)$ ) are bound states of  $b$  and  $\bar{b}$  quarks. An upsilon particle is decomposed into a  $b$  and  $\bar{b}$  pair in a hot QGP. The lighter of the three upsilon states has a deeper binding energy and is therefore more resistant to decomposition. Thus, the temperature of the QGP can be estimated by measuring the relative yield of the three Upsilon states produced within the QGP. The expected results of the upsilon measurement by the sPHENIX are depicted in Fig. 3. Here, upsilon particles are measured from their  $e^+e^-$  decays. Three upsilon states are clearly separated with designed momentum resolution of the sPHENIX detector system. Suppression of the peak(s) of the heavier upsilon provides a hint of the temperature of the QGP generated at the RHIC.

The RHIC is the only polarized proton collider in the world. By colliding polarized protons against each other at high energies, one can study how the spin of a proton is carried by its constituent quarks and gluons.

Prior to the RHIC, it was known that only 1/3 of the proton spin is carried by quark spin. Previous works at the RHIC have revealed that gluon spin also contributes to proton spin. However, the quark and gluon spins together do not appear to be sufficient to explain 100 % of the proton spin. If there is any remainder, it is the orbital angular momentum (OAM) of the partons within the proton. The sPHENIX will investigate the contribution of the OAM of partons in the proton spin, as illustrated in the bottom left image of Fig. 1.

---

<sup>\*1</sup> RIKEN Nishina Center

<sup>\*2</sup> Tokyo Metropolitan Industrial Technology Research Institute

<sup>\*3</sup> Center for High Energy and High Field Physics and Department of Physics, National Central University

<sup>\*4</sup> Department of Mathematical and Physical Sciences, Nara Women's University

<sup>\*5</sup> Japan Atomic Energy Agency

<sup>\*6</sup> Department of Physics, Korea University

<sup>\*7</sup> Department of Physics, National Taiwan University

<sup>\*8</sup> Department of Physics, Rikkyo University

<sup>\*9</sup> Physics Department, Brookhaven National Laboratory

<sup>\*10</sup> Department of Physics and Astronomy, Purdue University

<sup>a)</sup> The scientific illustration by Misaki Ouchida (Hokkaido University)

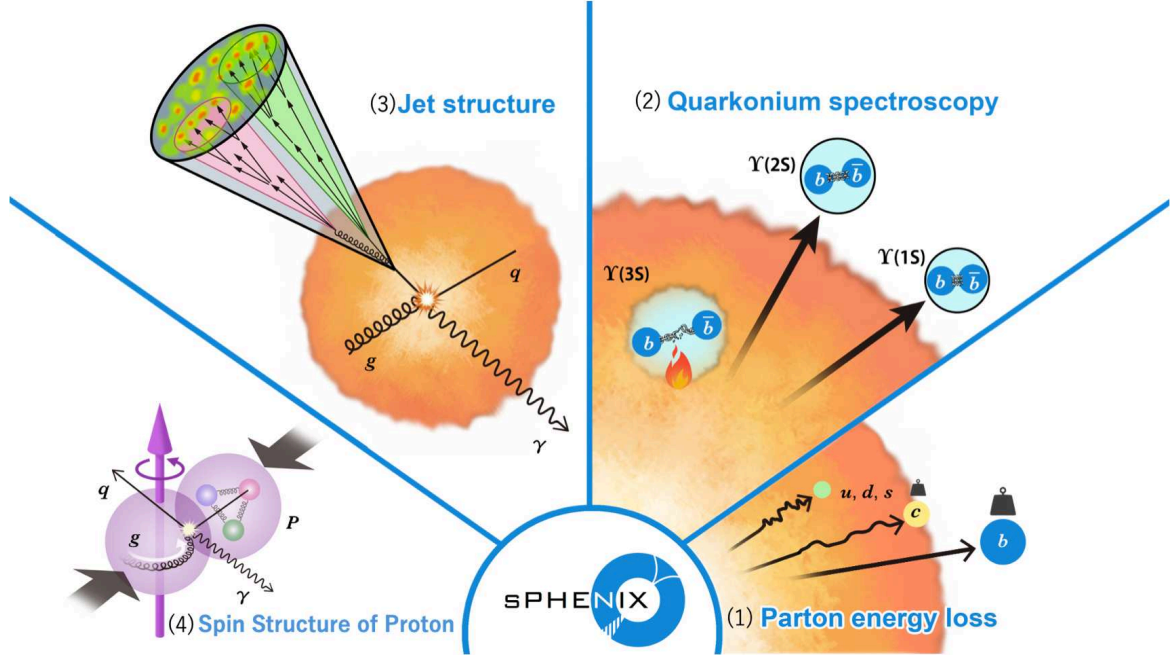


Fig. 1. Graphic sketches of physics goals of the sPHENIX.

## 2 sPHENIX Detector

The sPHENIX<sup>2)</sup> is a new state-of-art jet detector at the RHIC. The construction of the detector complex was completed by the end of April 2023 as shown in Fig. 4<sup>b)</sup>. The concept of sPHENIX follows the geometry of typical collider detectors, depicted in Fig. 5, covering the full azimuth and pseudo rapidity range of  $-1.1 \leq \eta \leq 1.1$ , with a tracking system consisting of a pixel detector (MVTX) based on monolithic ac-

tive pixel sensor technology, a silicon strip intermediate tracker (INTT), and a time projection chamber (TPC). The calorimeter stack includes a tungsten/scintillating fiber electromagnetic calorimeter (EMCAL) and a steel/scintillator tile hadronic calorimeter (HCAL), divided into inner and outer parts. The inner HCAL sits inside a 1.5 T superconducting solenoid, which was refurbished from the decommissioned BaBar detector<sup>5)</sup>.

b) Courtesy of Brookhaven National Laboratory

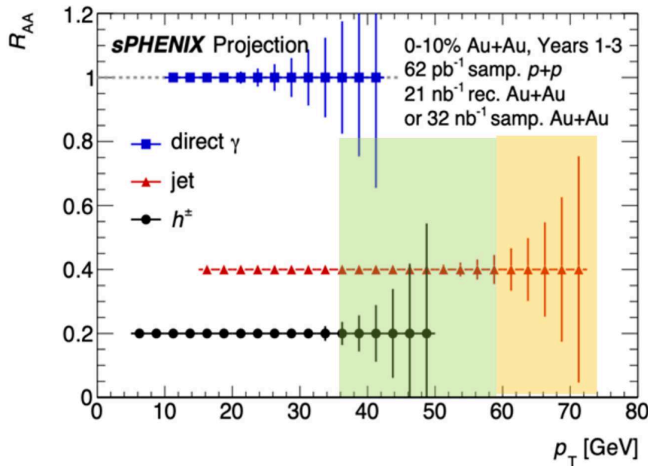


Fig. 2. Kinematic coverage in transverse momentum  $p_T$  of sPHENIX detector.<sup>1)</sup>

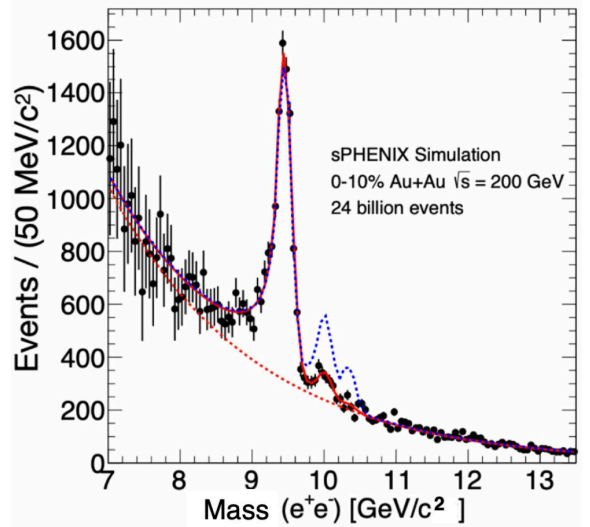


Fig. 3. Reconstructed invariant mass of  $e^+e^-$  pair in the central barrel region using Monte-Carlo simulated data.<sup>1)</sup>

The tracking system consisting of the MVTX, the INTT, and the TPC is the well-established detector formation of modern particle collider detectors such as STAR<sup>6)</sup> and ALICE.<sup>7)</sup> Each detector is excellent in position, timing, and momentum resolution, respectively and, thus, an essential component of a desirable high-energy collider detector.



Fig. 4. Photograph of the sPHENIX detector.

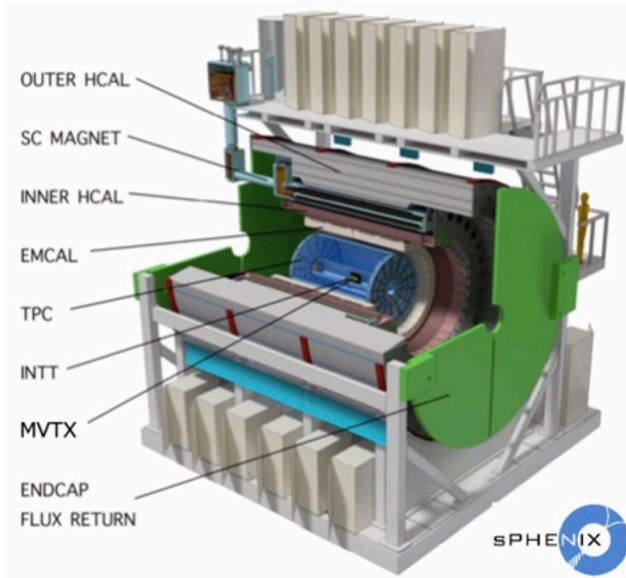


Fig. 5. The engineering drawing of the sPHENIX detector.

A minimum bias trigger is provided by the pair of minimum bias detectors (MBDs) implemented 2.5 m downstream of the collision point along a beam pipe in both directions. They are constructed from the reuse of the PHENIX beam-beam counter (BBC), consist-

ing of Čerenkov detectors made of a 3-cm-thick quartz radiator readout with mesh dynode photomultipliers. The collision vertex position along the beam axis is determined from the observed hit-timing difference between the MBD pair. The MBD has timing resolution of 50–60 ps for a single hit, which is translated to the reconstruction position resolution of  $< 2$  cm for proton+proton collisions and of few mm for Au+Au collisions. A pair of event plane detectors (EPD) is implemented further downstream of the MBD exploits 1.2-cm-thick scintillators with wavelength shifting fibers. Each EPD consists of two wheels of 12 sectors with 31 optically-isolated tiles. The EPD provides significant improvement in the event plane resolution of the Au+Au collision.

The data acquisition (DAQ) of the sPHENIX is designed to handle a trigger rate of 15 kHz. The Felix server system developed in ATLAS<sup>8)</sup> was employed as a part of the DAQ system for tracking detectors, which enables the processing of data in a stream readout mode as well.

### 3 INTT Silicon Detector and Japanese Contribution

The barrel-type INTT detector<sup>2)</sup> consists of the inner and outer layers of INTT ladders in the radius region of 7 to 10 cm from the beam line. The adjacent ladders are staggered against each other to prevent dead space between them and form inner and outer barrels from 24 and 32 ladders, as depicted in Fig. 6<sup>c)</sup>. Two silicon sensors and 26 readout chips<sup>d)</sup> are mounted on a high-density interconnect (HDI) flexible print cable forming a half INTT ladder. Two half-ladders are longitudinally aligned in parallel to the beam direction and glued on a supporting stave made of carbon fiber reinforced plastics (CFRP) as depicted in Fig. 7. Both glue and carbon fibers are high thermal conductive to diffuse heat generated by the readout chips. A water cooling system then removes the heat from the barrel through a carbon fiber tube implemented inside the body of the stave. The entire material budget of the INTT ladder in perpendicular direction is designed to be  $1\%X/X_0$ .

The strip-type silicon sensor has a strip width of  $78\ \mu\text{m}$ , length of 16 or 20 mm with thickness of  $320\ \mu\text{m}$ . The pulse generated in the silicon sensor is amplified and digitally converted in the adjacent readout chip. The digitized data are then transmitted downstream through the series of readout cables, which consisted of HDI, bus extender cable, and conversion cable. The HDI is a seven-layered flexible circuit cable and the line and space for low voltage differential signaling (LVDS)

c) Courtesy of Brookhaven National Laboratory

d) The chip is called FPHX and is designed to be low power consumption<sup>9)</sup>. It was invented for the forward vertex (FVTX) detector of PHENIX.





Fig. 6. INTT half barrels.

data lines are both  $60\ \mu\text{m}$ . The bus extender cable is a 1.1 m long flexible print cable employing liquid crystal as a dielectric material to suppress losses in transmission lines. The conversion cable consists of three components: 1)  $\mu$ -coaxial cables, 2) power and ground cables, 3) connector print boards both ends. The downstream of the conversion cable is connected to the read-out card (ROC), which collects data from multiple half-ladders and transmits reformatted data further downstream to the Felix server through an optical fiber link. The ROC was reused from the FVTX detector in the PHENIX experiment<sup>9)</sup> to reduce the cost of the INTT project.

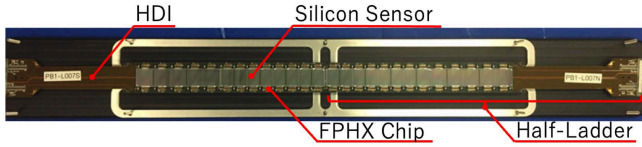


Fig. 7. Photograph of the INTT silicon ladder with sensors facing up.

Depicted in Fig. 8 is the INTT barrel detector installed inside the TPC detector. Because the entire INTT barrel needs to be accommodated within the inner diameter of the TPC, the signal from the barrel has to be transmitted all the way outside the TPC volume because the downstream electronics, that is, ROCs will not fit within the inner diameter of the TPC. The massive raw data generated from the INTT have to be transmitted at high speed to the ROC through a curved cable path for longer than 1 m. Because no commercial cable satisfies the requirement, a novel cable, that is, the bus extender cable has been developed based on flexible printed circuits. This technology can simultaneously satisfy high-density signal lines, length, and flexibility. The specification of the line and space of the bus extender of 120 and  $120\ \mu\text{m}$  prevents its

connector end design to be compatible with the input ports of the ROC. Therefore, another 15 to 25 cm adapter cable, that is, the conversion cable, was developed to interconnect between the bus extender and the ROC. To guide the connection smoothly without introducing any stress at the input connector of the ROC, flexibility in 3 dimensions for the conversion cable was required to absorb the geometrical mismatch of the downstream end of the bus extender and the corresponding input connector location of the ROC.

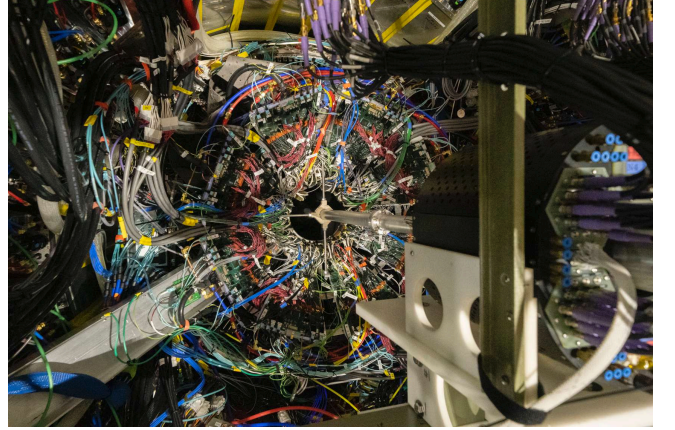


Fig. 8. The INTT barrel installed along the beam pipe.

The INTT detector was built as the in-kind contribution of RIKEN to the sPHENIX project. The entire INTT project was thus conducted mainly by RIKEN and Japanese collaborators. Most of the detector components were produced in Japan, as the major R&D works were carried out there. The Japanese INTT collaboration mainly consisted of RIKEN, Nara Women's University, Rikkyo University, and Japan Atomic Energy Agency. As displayed in Fig. 9, about half of the INTT collaboration is occupied by Japanese collaborators. The module assemblies were carried out in Taiwan and BNL.

#### 4 Run23 Performance

The very first beam commissioning of the sPHENIX detector took place using Au+Au collision at  $\sqrt{s_{NN}} = 200\ \text{GeV}$  (Run23) following the completion of the construction. The result of quick analyses during the commissioning period for selected subsystem detector performance are presented in this section. Further details are discussed elsewhere<sup>11)12)</sup>. The calorimeters achieved quite high live regions as displayed in Fig. 10. The figure exhibits the event display of the EMCAL, inner and outer HCALS observed in a high-multiplicity event in the Au+Au collision. The reconstructed invariant mass of di-photon pairs observed by the EMCAL is depicted in Fig. 11. Although there is still room for improvement in energy calibration, the  $\pi^0$  peak is

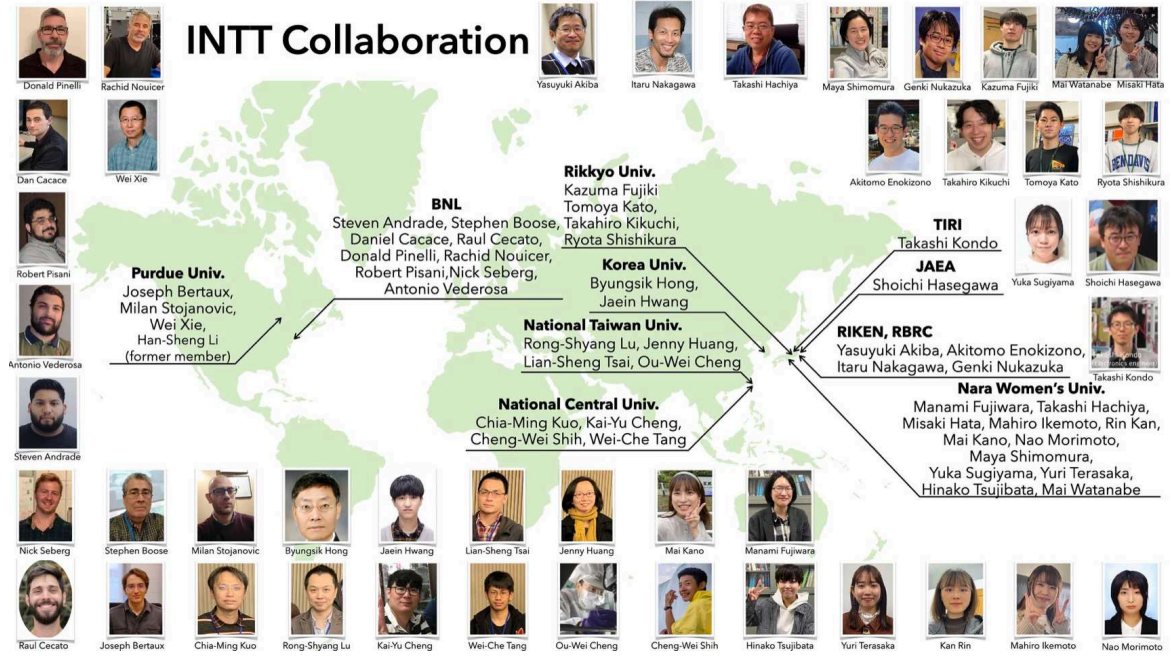


Fig. 9. The INTT collaboration.

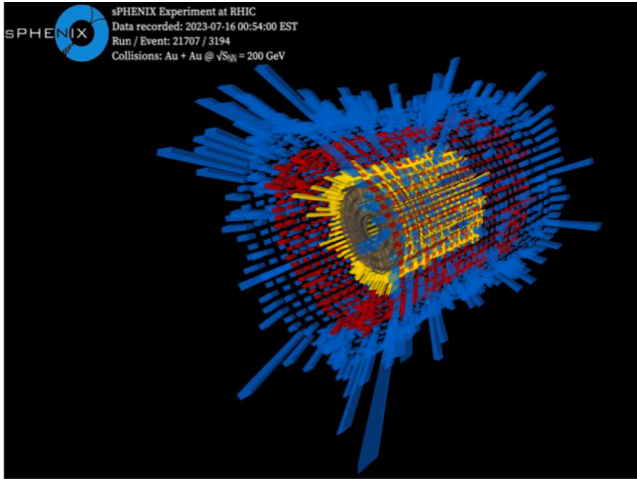


Fig. 10. Event display of the EMCAL (yellow), the Inner (red), and the Outer (blue) HCAL observed in  $\sqrt{s} = 200$  GeV Au+Au collision. The length of the bar is proportional to the energy deposit measured by each calorimeter tower.

visible at approximately the 100<sup>th</sup> ADC channel, which implies that the EMCAL is functioning properly.

The commissioning of tracking detectors was also pursued in parallel to that of calorimeters. The INTT detector was successfully commissioned as well as other subsystem detectors and appeared in 98% channels alive amongst 373k total channels. The signals observed by the INTT detector were certainly corre-

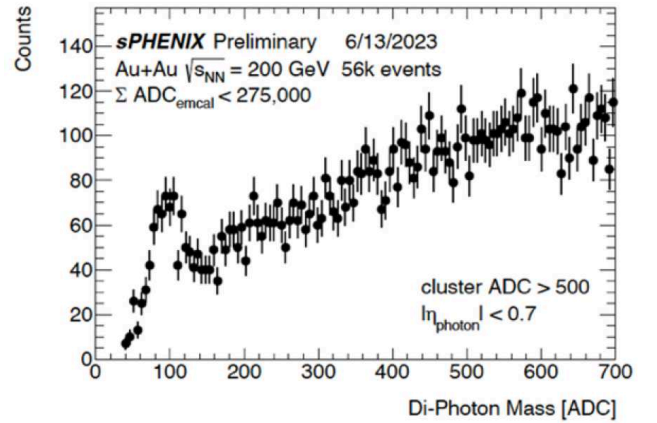


Fig. 11. Reconstructed invariant mass distribution from observed di-photon pairs in the EMCAL. The peak at approximately the 100<sup>th</sup> channel in the ADC unit corresponds to  $\pi^0$ .

lated with a given collision, which can be proven by a clear correlation in the multiplicity with other detectors. Figure 12 is the correlation between the number of hit clusters in the INTT and the total charge observed in the MBD (the total charge is proportional to the number of particles). The crucial feature of the INTT, that is, the timing resolution was demonstrated to be achieved approximately 200 ns, which can identify INTT hits within every other beam bunch crossings. The ultimate requirement is better than one

beam bunch crossing (106 ns) for the INTT, which can be achievable by removing timing jitters between the FELIX servers. The solution of upgrading the firmware has already been carried out and to be verified once we start collecting data of proton+proton collision starting in May, 2024. The INTT and other subsystem detectors thus demonstrated excellent performance and accumulated reasonably high-quality data even in the commissioning period. Certain working groups have been launched for several physics topics aiming for physics publications in ambition from Run23 data. The INTT was one of the most advanced subsystem detectors in Run23 commissioning. We are ambitious to publish the analysis results of the charged particle distribution as a function of rapidity ( $dN/d\eta$ ) using the INTT tracklets.

- 9) C. Aidala *et al.*, Nucl. Instr. Meth. **A 755**, 44 (2014).
- 10) T. Kondo *et al.*, Journal of The Japan Institute of Electronics Packaging, **15**, E21-007-1 (2022).
- 11) I. Nakagawa, *et al.*, in this report.
- 12) G. Nukazuka, *et al.*, in this report.

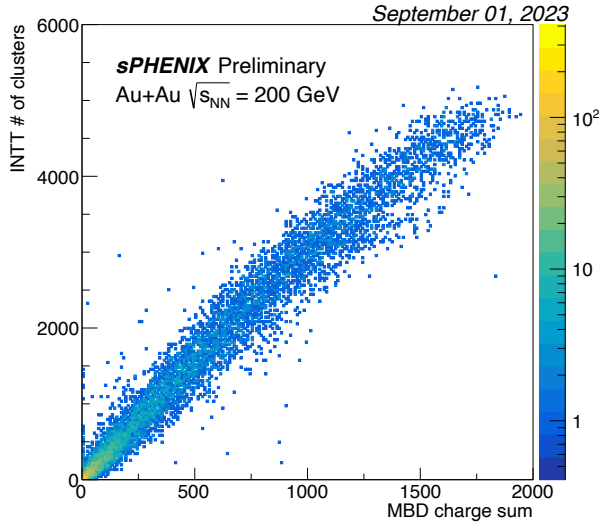


Fig. 12. Hit multiplicity correlation between the INTT and the MBD detectors. The vertical axis indicates the number of clusters of the INTT hits and the horizontal axis indicates the observed total charge sum in the MBD crystals.

#### References

- 1) An Upgrade Concept from the PHENIX Collaboration, arXiv:1207.6378v2 (2012).
- 2) Technical Design Report of sPHENIX (2019). <https://indico.bnl.gov/event/7081/>
- 3) K. Adcox *et al.*, Nucl. Instr. Meth. **A 499**, 469 (2003).
- 4) Nikkei Science, June (2023).
- 5) Nucl. Instr. Meth. **A 479**, 1 (2002).
- 6) M. Anderson *et al.*, Nucl. Instr. Meth. **A 499**, 659 (2003), G. Contin *et al.*, arXiv:1710.02176 [physics.ins-det] (2018).
- 7) The ALICE Collaboration, CERN-LHCC-2012-013 / LHCC-P-005, ALICE-UG-002 (2012).
- 8) M. Wu (ATLAS TDAQ Collaboration), Nucl. Instr. Meth. **A 1048**, 167994 (2023).